Title

Identification of a First-in-Class Small-Molecule Inhibitor of the EIF4E-RBM38 Complex That Enhances Wild-type TP53 Protein Translation for Tumor Growth Suppression.

Journal

Molecular Cancer Therapeutics, 22(6)

ISSN

1535-7163

Authors

Lucchesi, Christopher A

Zhang, Jin

Gao, Mingchun

et al.

Publication Date

2023-06-01

DOI

10.1158/1535-7163.mct-22-0627

Peer reviewed

HHS Public Access

Author manuscript

Mol Cancer Ther. Author manuscript; available in PMC 2024 February 14.

Published in final edited form as:

Mol Cancer Ther. 2023 June 01; 22(6): 726–736. doi:10.1158/1535-7163.MCT-22-0627.

Identification of a First-in-Class Small Molecule Inhibitor of the eIF4E-RBM38 Complex that Enhances wild-type p53 Protein Translation for Tumor Growth Suppression

Christopher A. Lucchesi[1,*], **Jin Zhang**[1], **Mingchun Gao**[2], **Jared Shaw**[2], **Xinbin Chen**[1,*]

[1]Comparative Oncology Laboratory, Schools of Veterinary Medicine and Medicine, University of California at Davis, Davis, California

[2]Department of Chemistry, University of California, Davis, Davis, California

Abstract

eIF4E, an mRNA cap-binding protein, is necessary for cap-dependent translation. Overexpression of eIF4E is known to promote cancer development by preferentially translating a group of oncogenic mRNAs. Thus, 4EGI-1, a disruptor of eIF4E-eIF4G interaction, was developed to inhibit oncoprotein expression for cancer therapy. Interestingly, RBM38, an RNA-binding protein, interacts with eIF4E on p53 mRNA, prevents eIF4E from binding to p53 mRNA cap, and inhibits p53 expression. Thus, Pep8, an eight amino acid peptide derived from RBM38, was developed to disrupt the eIF4E-RBM38 complex, leading to increased p53 expression and decreased tumor cell growth. Herein, we have developed a first-in-class small molecule compound 094, which interacts with eIF4E via the same pocket as does Pep8, dissociates RBM38 from eIF4E, and enhances p53 translation in RBM38- and eIF4E-dependent manners. Structure-activity relationship (SAR) studies identified that both the fluorobenzene and ethyl benzamide are necessary for compound 094 to interact with eIF4E. Further, we showed that compound 094 is capable of suppressing 3D tumor spheroid growth in RBM38- and p53-dependent manners. Additionally, we found that compound 094 cooperates with chemotherapeutic agent doxorubicin and eIF4E inhibitor 4EGI-1 to suppress tumor cell growth. Collectively, we showed that two distinct approaches can be used together to target eIF4E for cancer therapy by enhancing wild-type p53 expression (094), and by suppressing oncoprotein expression (4EGI-1).

Keywords

eIF4E; p53; Small molecule inhibitor; RBM38

Introduction

Translation control is a tightly regulated process that plays a major role in cell growth, differentiation, and proliferation. The process of translation is broken up into four consecutive stages, including initiation, elongation, termination and ribosome recycling.

*Correspondence to: Christopher A. Lucchesi, calucchesi@ucdavis.edu, Xinbin Chen, xbchen@ucdavis.edu.

The authors declare no potential conflicts of interest

The eukaryotic translation initiation factor 4E (eIF4E) protein is the rate-limiting factor in the formation of eIF4F complex, and consequently, plays a critical role in the regulation of translation initiation rates[1]. As one of the least abundant translation factors, eIF4E accessibility is controlled at multiple levels including transcriptionally, post-transcriptionally, post-translationally and through inhibitor protein-protein interactions (4E-binding proteins (4E-BPs))[2][3]. This stringent modulation of eIF4E offers an apparatus to moderate translational rates in response to stress conditions, including oncogenic stimulation[4]. However, research conducted over the past decades have clearly established that over activity of eIF4E can be a principal source for various diseases, including cancer[5].

Numerous studies have shown that elevated levels of eIF4E protein enhance cell transformation, tumorigenesis, metastasis, and drug resistance in both experimental cancer models and human cancer tissues[6–9]. Furthermore, elevated eIF4E function was found to selectively and disproportionately enhance the translation of mRNAs encoding for potent growth and survival factors particularly involved in tumorigenesis[6]. These oncogenic mRNA have long 5′ untranslated regions coupled with high G/C content which results in these transcripts forming complex hairpin structures that necessitates eIF4A helicase activity to allow for scanning of the 40s ribosomal subunit. As eIF4E is a potent enhancer of eIF4A helicase activity[10], these poorly translated “weak” mRNA rely heavily on enhanced eIF4E expression/activity[11]. Therefore, within the oncogenic stimuli framework, “weak” mRNA receive enhanced translational efficiencies through the hyperactivity of eIF4E ultimately leading to tumorigenesis.

It is therefore no surprise that a substantial amount of effort has been put forth to identify ways to modulate eIF4E activity as a potential therapeutic tactic. To date, the two most common approaches have been to use m^7G cap analogs, such as the pro-drug 4Ei-1, to block eIF4E ability to bind target mRNA, or block eIF4E ability to interact with eukaryotic initiation factor 4G (eIF4G), necessary for the formation of the eIF4F complex, using small molecule compounds like 4EGI-1[12–15]. These approaches have shown to be effective at decreasing the translation of pro-oncogenic transcripts leading to decreased tumor cell growth [5,16]. Contrastingly, our group has worked on enhancing the translation of the key tumor suppressor p53 by inhibiting the translation repression of p53 by the RNA-binding protein RBM38.

Previously, our group discovered that RBM38 inhibits p53 translation via interacting with eIF4E and p53 mRNA, effectively preventing eIF4E from binding to p53 m^7G cap halting its translation[17]. With therapeutic relevance, we found that abrogating the ability of RBM38 to bind to eIF4E using short inhibitory peptides (Pep7 or Pep8) induced wild-type p53 expression, and sensitized cancer cells to doxorubicin and radiotherapy[18,19]. The p53 transcription factor functions as a critical tumor suppressor and principal regulator of many signaling pathways involved in numerous aspects of tumor suppression. Activated p53 induces multiple antiproliferative apparatuses by moderating expression of genes involved in DNA repair, cell cycle arrest, apoptosis, and senescence[20]. Therefore, activation of wild-type p53 by targeting non-genetic mechanisms, such as RBM38 that inhibits p53 translation, is a promising therapeutic tactic for malignancies that carry wild-type p53. Replica exchange

molecular dynamic simulations (REMDS) combined with site-directed mutagenesis assays demonstrated that Pep7 and Pep8 bind to eIF4E via a previously undrugged C-terminus pocket forming a key hydrogen bond with eIF4E aspartic acid 202[18,19]. With this knowledge, we sought to discover a first-in-class small molecule inhibitor of the eIF4E-RBM38 complex to enhance p53 protein expression as a therapeutic approach for cancers that harbor wild-type p53 expression. We ultimately discovered that compound 094 is a potent inhibitor of the eIF4E-RBM38 complex leading to enhanced p53 protein expression, decreased 3D tumor spheroid cell viability, and enhanced sensitivity to doxorubicin in RKO and HCT116 colon cancer cells. Furthermore, we showed that 094 further sensitized RKO cancer cells to the eIF4E translation inhibitor 4EGI-1. This data supports that inhibiting the selective translation of oncogenic transcripts with 4EGI-1, while enhancing the translation of the p53 tumor suppressor with compound 094, may be an effective therapeutic strategy.

Materials and Methods

Compound synthesis

For compound 094, and other derivatives that were not commercially available, the synthesis and characterization can be found in the supplemental methods section. The compound name, structure and chemical name of all compounds used can be found in supplemental table 1.

Plasmids and cell line generation

Generation of the RBM24 and RBM38 double knockout cell line was performed by knocking out RBM24 in RBM38-null cell lines as previously described[18]. Briefly, RBM24 knockout cell lines were generated by CRISPR-cas9 genome editing method. sgRNAs targeting RBM24 were designed using the CRISPR design tool and cloned into the BbsI sites of CRISPR vector pSpCas9(BB)-2A-Puro. Two specific gRNAs were used: gRNA #1 GTA CAC CAA GAT CTT CGT CG and gRNA #2 CGA GGT CTT CGG CGA GAT CG. The cells were selected with puromycin and each individual clone was confirmed by western blot and sequencing analysis. Generation of p53-null knockout cell lines were generated by CRISPR-cas9 genome editing method. sgRNAs targeting p53 were designed using the CRISPR design tool and cloned into the BbsI sites of CRISPR vector pSpCas9(BB)-2A-Puro. Two specific gRNAs were used: gRNA #1: 5′-CCA TTG TTC AAT ATC GTC CG, gRNA #2: 5′-TCC ATT GCT TGG GAC GGC AA. The cells were selected with puromycin, and each individual clone was confirmed by Western blot analysis. Generation of HCT116 eIF4E D-202-K and eIF4E ΔC cells lines was as previously described[21].

GST-RBM38 expression plasmid was generated as previously described[22]. pTXB1-eIF4E plasmid was generated by amplifying eIF4E using His-eIF4E expression plasmid as template. The amplicon was then cloned into pTXB1 via NdeI and SapI. The primers used to amplify eIF4E were forward primer, 5′-GGT GGT CAT ATG GCG ACT GTC GAA CCG GAA ACC-3′, and reverse primer, 5′-GGT GGT TGC TCT TCC GCA AAC AAC AAA CCT ATT TTT AGT GGT GGA G-3′. pCDNA4-Avi-eIF4E (Avi-tagged-eIF4E) plasmid was generated by amplifying eIF4E using His-eIF4E expression plasmid as template. The

amplicon was then cloned into pCDNA4 mammalian vector via BamHI and NotI. The primers used to amplify eIF4E were forward primer, 5´- ATCGTA GGATCC GCCACC ATG GGC CTG AAC GAC ATC TTC GAG GCC CAG AAG ATC GAG TGG CAC GAG ATG GCG ACT GTC GAA CCG-3´, and reverse primer, 5´- TAC GAT GCG GCC GC CTA AAC AAC AAA CCT ATT TTT AGT GGT GGA-3´.

Photoaffinity Assay

This method was adopted from Kumar et al.,[23]. Briefly, 094 was synthesized with a 3*H*-diazirine to generate our photoprobe. Bacterial purified eIF4E was split into two fractions and then incubated with the 094-photoprobe in the dark for 30 min. Next, one sample was subjected to UV light (λ_{ext} = 320–400 nm) for 10 minutes while the other sample was kept in the dark. Finally, eIF4E was acetone precipitated, trypsin digested and subsequently analyzed by liquid chromatography mass spectrometry.

Biolayer interferometry (BLI)

BLI experiments were performed on an Octet RED96 instrument (ForteBio, Menlo Park, California) that can simultaneously monitor eight samples in parallel. HCT116 cells were co-transfected with pCDNA4-Avi-eIF4E and bacterial biotin ligase plasmid pCDNA4-Bira-HA for 24 hours. Cells were lysed in PBST with protease inhibitor cocktail followed by sonication (five seconds on, 15 seconds off, for five pulses). Streptavidin biosensor tips were used to load Avi-eIF4E before testing the binding affinity of peptides or small molecule. Octet measurements were carried out at 22°C and shaken at 1,000 rpm.

Human cell lines

Cell lines HCT116 (RRID:CVCL_0291) and RKO (RRID:CVCL_0504) were obtained from ATCC between 2007 and 2016 and used below passage 25 or within 2 months after thawing. Cells were tested negative for mycoplasma after thawing and used within two months. Since all cell lines from ATCC have been thoroughly tested and authenticated, we did not authenticate the cell lines used in this study. HCT116 and RKO colon cancer cells were cultured at 37°C in DMEM (Dulbecco’s Modified Eagle’s medium, Invitrogen) supplemented with 10% fetal bovine serum (Hyclone, Logan, UT, USA) in a humidified incubator with 5% CO_2.

Competitive ELISA

Briefly, bacterially purified GST-tagged RBM38 protein was incubated in a 96-well glutathione coated plate. After washing, equal amounts of purified eIF4E protein was added to each well with or without small molecule inhibitors. Finally, each well was extensively washed and incubated with HRP-conjugated eIF4E antibody before being visualized with TMB substrate solution.

RNA isolation, RT-PCR, and quantitative RT-PCR

Total RNA was isolated with Quick-RNA Miniprep Kit (Zymo Research). cDNA was synthesized using RevertAid First Strand cDNA Synthesis kit according to the manufacturer’s protocol (ThermoFisher Scientific). For qRT-PCR analysis, 20 μL reactions

were set up using 2x qPCR SYBR Green Mix (ABgene) along with 5 μmol/liter primers. The reactions were run on a StepOne plus (Invitrogen) using a two-step cycling program: 95 °C for 15 min, followed by 40 cycles of 95 °C for 15 s, 60 °C for 30 s, and 68 °C for 30 s. A melt curve (57–95 °C) was generated at the end of each run to verify primer specificity. The primers used to amplify human HPRT1 were forward primer 5'-TAT GGC GAC CCG CAG CCC T-3', reverse primer 5'-CAT CTC GAG CAA GAC GTT CAG-3'. The primers used to amplify p53 were forward primer 5'- CCT CAG CAT CTT ATC CGA GTG G-3', and reverse primer 5'- TGG ATG GTG GTA CAG TCA GAG C-3'. The primers used to amplify p21 were forward primer 5'- AGG TGG ACC TGG AGA CTC TCA G-3', and reverse primer 5'- TCC TCT TGG AGA AGA TCA GCC G-3'. The primers used to amplify PUMA were forward primer 5'- ACG ACC TCA ACG CAC AGT ACG A-3', and reverse primer 5'- CCT AAT TGG GCT CCA TCT CGG G-3'.

RNA-ChIP assay

RNA immunoprecipitation was carried out as previously described[18]. Cell extracts were prepared with immunoprecipitation buffer (10 mM HEPES, pH 7.0, 100 mM KCl, 5 mM MgCl2, 0.5% Nonidet P-40, and 1 mM DTT) and then incubated with 1 μg of anti-eIF4E (Anti-eIF4E Antibody (A-10), Santa Cruz Biotechnology) or an isotype control IgG overnight at 4 °C. The RNA–protein immunocomplexes were brought down by magnetic protein A/G beads. RT-PCR analysis was carried out to determine the levels of p53 and HPRT1 (used as a control) transcripts.

Western blot analysis

Western blot procedures were as previously described[24]. Briefly, cell lysates were resolved in 8–12% SDS-polyacrylamide gel and then transferred to nitrocellulose membranes. Blots were blocked in PBST containing 3% milk for 1 hour at 20°C. Primary antibodies in PBST containing 3% milk were incubated at 4°C rocking overnight. The following morning membranes were washed 3x with PBST followed by the addition of secondary antibody in PBST containing 3% milk at 20°C for 2 hours. Membranes were then washed 3x with PBS. Band intensities were calculated using ImageJ [25]. Antibodies used are: anti-p53 (Cell Signaling Technology Cat# 2524, RRID:AB_331743), anti-actin (Sigma-Aldrich Cat# A2228, RRID:AB_476697, used as loading control), anti-GST (Santa Cruz Biotechnology Cat# sc-138, RRID:AB_627677), anti-eIF4E (Santa Cruz Biotechnology Cat# sc-9976, RRID:AB_627502), anti-Vinculin (Santa Cruz Biotechnology Cat# sc-73614, RRID:AB_1131294, used as loading control), anti-GAPDH (Santa Cruz Biotechnology Cat# sc-47724, RRID:AB_627678, used as loading control) and anti-phospho-histone H2A.X (Ser139) (Cell Signaling Technology Cat# 9718, RRID:AB_2118009), anti-cleaved caspase 3 (Cell Signaling Technology Cat# 9664, RRID:AB_2070042), anti-cleaved PARP (Cell Signaling Technology Cat# 5625, RRID:AB_10699459). Anti-RBM38 antibody was made as described previously[22] .

Nascent protein detection with Click-iT chemistry

Wild-type and eIF4E Δ-Cterm HCT116 cells were plated in duplicate at 2.5×10^6 cells per 10 cm plate. The next day the cells were washed three times with methionine free DMEM and then treated with Click-it HPG (ThermoFisher, C10186) and DMSO ctrl or

094 (10 μM) in methionine free DMEM for 2 hours. The cells were then washed three times with PBS and collected via trypsinization. The pelleted cells were then lysed in 750 μL lysis buffer (25 mM Tris pH 8.0, 100 mM NaCl, and 0.1% Triton X-100) including protease inhibitor cocktail. The homogenized pellets were then subjected to sonication on ice (5 seconds on, 15 seconds off, for 5 pulses). After lyses, the cells were pelleted and lysate was collected in new tubes. 50 μL from each tube was removed to be used for the input. Next, 15 μL protein A/G magnetic beads were added to each tube followed by 1 μg p53 (Santa Cruz Biotechnology Cat# sc-126, RRID:AB_628082) antibody. After rocking overnight at 4°C the beads were washed 5 times before being subjected to Click-it biotin assay (including the input samples) utilizing Click-iT Protein Reaction Buffer Kit (Invitrogen, C10276) according to manufactures protocol. Nascent protein expression was visualized by western-blot using anti-biotin antibody (Santa Cruz Biotechnology Cat# sc-57636, RRID:AB_628778).

Competitive pull-down assays

For the GST-RBM38 competitive pull-down assays it was performed as previously described[26]. Briefly, pGEX-4T3-RBM38 plasmid was transformed into BL21 (DE3) competent E. coli. 1-liter culture was grown at 37°C until OD600 = 0.6–0.8 and then induced with a final concentration of 0.1 mM IPTG for 4 hours. Bacteria were pelleted and then placed in −80°C overnight. Pellets were lysed, sonicated, and centrifuged in 20 mL lysis buffer (50mM Tris pH 7.5, 150mM NaCl and 0.1% Triton X-100) supplemented with benzonase, 1 mM DTT and protease inhibitor cocktail. Lysates were then incubated with GST beads rocking at 4 °C for 2 hours. Beads were washed 3x with lysis buffer. After brief centrifugation, lysates were carefully removed. Beads were then resuspended in lysis buffer with 0.1% Triton X-100 to make a 50% bead slurry. 100 μL bead slurry was incubated in 830 μL lysis buffer, 20 μM (20uL) peptide (Ctrl or Pep8) or 20 μM compound (094 or 117) and 250ug (50uL) purified eIF4E in a 1.5 mL tube. Samples were rocked overnight, washed 3x with lysis buffer and eluted with 60 μL 1x SDS-loading buffer before western blot analysis.

2-D Cell Viability Assay

For 2-D cell viability assays, 10,000 cells per well were plated in a triplicate in a 96 well plate. Two hours later, small molecule compounds or DMSO control were added to each well. Twenty-four hours later, cell viability was measured by CellTiter-Glo 3D according to manufacturer’s guidelines (Promega).

3-D Organoid Cultures

3-D mini ring culture assays were adapted from Phan et al.,[27]. Briefly, single cell suspensions (15K cells/well) were plated around the rim of the well in 96-well plates in a 4:3 mixture of Matrigel and Mammocult (BD Bioscience CB-40324). After plates were incubated at 37°C with 5% CO2 for 15 min to solidify the gel, 100 μL of prewarmed Mammocult containing the indicated small molecule or DMSO control was added to the corresponding well. Seventy-two hrs later, 100 μL pre-warmed PBS was used to wash the cells 3 times. Cells were then released from the Matrigel by incubating at 37°C for 45 min in 50 mL of 5 mg/mL dispase (Life Technologies #17105–041). Images were taken

with a 10x objective and then cell viability was measured by CellTiter-Glo 3D according to manufacturer's guidelines (Promega).

Statistical analysis

Experimental values are presented as mean ± SEM. Statistical comparisons between experimental groups were analyzed by two-way ANOVA or two-tailed Student's t-test where appropriate. P values < 0.05 were considered statistically significant.

Data Availability

The data generated in this study are available upon request from the corresponding author.

Results

Identification of the eIF4E-RBM38 inhibitor 094.

Previously, we determined that RBM38, and its homologous family member RBM24, directly interact with eIF4E on the p53 transcript resulting in the dissociation of eIF4E from the 5′-cap, thereby suppressing p53 translation[17,28]. Furthermore, we showed that Pep8, a synthetic peptide derived from the carboxyl-terminus of RBM38, abrogates the eIF4E-RBM38 complex enhancing p53 translation leading to tumor xenograft growth suppression and sensitization to doxorubicin[18]. To identify a first-in-class small molecule inhibitor of the eIF4E-RBM38 complex, our workflow started by performing an *in-silico* virtual screen of the ZINC database "clean lead-like subset" (Fig. 1A)[29]. We preferentially screened for small molecules that docked within the previously identified Pep8 binding site on eIF4E (Fig. 1B, upper panel)[18]. To further refine our search for drug-like compounds, we focused on compounds that conformed to two of Lipinski's "rule of five", i.e., a calculated log P (Clog P) greater than 1, but less than 5, and a molecular mass less than 500[30]. Using AutoDock Vina, we designed a search grid concentrated around an area within 5 Å from the previously identified Pep8 binding site[18]. After docking, the results were evaluated by ranking the various complexes toward their predicted binding energies. We further narrowed the top 100 potential leads by screening for compounds that were within three angstrom distance from eIF4E Asp:202, which is known to directly contact the serine residue in Pep8 [18]. From this initial screen, we identified compound 094, which was predicted to bind within the same pocket as Pep8 on eIF4E (Fig. 1B, lower panel).

To investigate the binding interface between 094 and eIF4E, and to confirm our initial *in-silico* screen, we utilized a photoaffinity labeling (PAL) approach[31] as outlined in figure 1C. We first synthesized 094 with a UV light activated 3*H*-diazirine to generate our photoprobe. Equal amounts of bacterial purified human eIF4E protein were incubated with 094-photoprobe and split into two sample groups (one treated with UV light, and one kept in the dark). Each sample was then subjected to LC-MS/MS to see where/if 094 bound to eIF4E. Upon subtracting the mass of the denitrogenated 094-photolabel, we confirmed that 094 bound within the predicted C-terminus binding pocket in eIF4E corresponding to amino acid residues 174–211 (Figure 1D–E, purple fragments). Collectively, these results indicate that compound 094 directly interacts with eIF4E via a previously undrugged C-terminal pocket.

Compound 094 dissociates the eIF4E-RBM38 complex

With confirmation that 094 binds to eIF4E via its C-terminus pocket, we next sought to determine the equilibrium dissociation constant (K_D) for 094 to purified eIF4E protein using bio-layer interferometry (BLI). Our previously evaluated Pep8 peptide was used as a positive control, which had a K_D of 25 μM, whereas 094 was found to have a K_D of 16 μM (Fig. 2A), supporting that 094 has a stronger affinity for eIF4E than does Pep8.

We next questioned if 094 is capable of disrupting the eIF4E-RBM38 complex. To that end, we utilized a competitive pull-down assay. GST-tagged RBM38 was bound to GSH-magnetic beads and then incubated with purified eIF4E with either positive control Pep8 peptide, or with compound 094. We found that 094 had a stronger ability to suppress the eIF4E-RBM38 complex as compared to Pep8 peptide (Fig. 2B, compare lanes 2 and 4), consistent with the observation by BLI analysis (Fig. 2A). Collectively, these data support that 094 is a more potent inhibitor of the eIF4E-RBM38 complex than Pep8.

Compound 094 modulates p53 protein expression

We previously demonstrated that the Pep8 peptide enhances p53 proteins expression through abrogating the interaction between RBM38 and eIF4E. As compound 094 disrupts the eIF4E-RBM38 complex, we next asked whether 094 is also able to enhance p53 protein expression. Indeed, we found that compound 094 was a more potent inducer of p53 protein expression than the Pep8 peptide (Fig. 3A, compare lanes 2 and 4). Next, we questioned the specificity of compound 094. To that end, wild-type and RBM24/RBM38-null RKO cells were treated with escalating doses of 094. Western-blot analysis revealed that 094 enhanced p53 protein expression in a dose-dependent manner in wild-type cells, but failed to do so in the RBM24/RBM38-null cells, suggesting target specificity (Fig. 3B).

Since p53 is known to be sensitive to a multitude of stresses, we wanted to confirm that the ability of 094 to enhance p53 translation is due to its ability to interact with eIF4E and not potential off-target cytotoxicity. *In silico* modeling demonstrated that a key halogen bond between compound 094 and Asp:202 in eIF4E is necessary for their interaction (Supp. Fig. 1A). Suggestively, this interaction may be disrupted by substituting the negatively charged aspartic acid with a positively charged lysine. Therefore, two eIF4E mutant HCT116 cell lines[21], eIF4E D-202-K in that Asp202 was substituted with lysine, and eIF4E Δ-Cterm in that the C-terminal 17 amino acids (amino acids 201–217) were deleted, were used to further address the specificity of compound 094. *In-silico* modeling showed that eIF4E Δ-Cterm mutant has lost the binding pocket necessary for 094 interaction (Supp. Fig. 1B). As a control, we showed that 094 enhanced p53 expression in wild-type HCT116 cells in a dose dependent manner but failed to do so in RBM38-null cells (Fig. 3C). Furthermore, we showed that 094 failed to enhance p53 expression in both eIF4E mutant cell lines (Fig. 3C). These data support that compound 094 specifically interacts with eIF4E to enhance p53 protein expression.

To determine whether 094 enhances p53 expression through enhancing its mRNA translation, we first looked at the levels of p53 mRNA and p53 downstream targets p21 and PUMA in wild-type and RBM24/RBM38-null RKO cells mock-treated or treated with

094. We showed that 094 treatment did not enhance p53 mRNA expression in wild-type cells, whereas both p21 and PUMA transcripts were increased (Fig. 3D). Additionally, we found that none of the transcripts were increased in the RBM24/RBM38-null cells, further supporting 094 target specificity (Fig 3D). We would like to mention that loss of RBM24/RBM38 had no effect on p53 mRNA levels (Suppl. Fig. 1C). We previously demonstrated that Pep8 blocks RBM38 from interacting with eIF4E, thereby enhancing eIF4E ability to interact with p53 mRNA leading to enhanced p53 mRNA translation[18]. Therefore, we performed an RNA-ChIP assay in RKO cells treated with 094 and found that 094 treatment enhanced the ability of eIF4E to interact with p53 mRNA (Fig. 3E). Further, we found that 094 enhanced p53 *de-novo* protein expression in wild-type, but not in eIF4E Δ-Cterm HCT116 cells (Fig. 3F). We would like to mention that basal p53 *de-novo* protein expression was higher in the eIF4E Δ-Cterm HCT116 cells, supporting our previous observation that RBM38 is unable to bind this truncated eIF4E protein, enhancing p53 translation[21]. Lastly, we determined that 094 was unable to enhance p53 protein stability (Supp. Fig. 2). Collectively, these data support that 094 exerts its mode of action by binding with eIF4E, limiting the interaction between eIF4E and RBM38, thereby enhancing p53 mRNA translation.

Structure-activity relationship of compound 094

To probe 094 structure-activity relationship (SAR), we assayed structural variants of 094. In an effort to mitigate identifying false positive compounds, we devised a competitive ELISA assay in which the ability for a compound to dissociate eIF4E from RBM38 could be measured directly (Fig. 4A). First, we tested the chirality of compound 094 by asking which enantiomer (R or S) retained activity (Fig. 4B). Our competitive ELISA for the 094 R and S enantiomers showed that neither had enhanced or diminished activity (Fig. 4C). We confirmed via western blot that both enantiomers were able to enhance p53 protein expression, suggesting no difference in chirality (Fig. 4D). Consequently, the subsequent studies were performed using a racemic mixture of the 094 analogs.

Next, we performed a two-dose escalation test of all 094 derivatives to identify potential candidates with enhanced activity (structures in Supp. Fig. 3A). We found that besides compound 094, only compound 117 had a substantial dose response, whereas compounds 123, 170, 603 and 097 had a minimal activity (Supp. Fig. 3B). This initial SAR revealed that both the fluorobenzene and ethyl benzamide play key roles in the binding to eIF4E C-terminus pocket. We next assayed whether compounds 097 or 117 had enhanced activity over 094 at higher molar ratios (structures shown in figure 4E). This competitive ELISA demonstrated that compound 117 had similar efficacy at 1:1 and 2:1 molar ratios (drug/eIF4E), but modestly lower efficacy at 3:1 molar ratio (Fig. 4F). We further confirmed that compound 117, like 094, was able to dissociate eIF4E from RBM38 by performing GST-tagged RBM38 GST-pulldown assay (Supp. Fig. 3C). Together, these data demonstrate that compounds 094 and 117 are potent inhibitors of the eIF4E-RBM38 complex.

094 inhibits tumor cell growth and enhances doxorubicin-mediated growth suppression

To understand if the increased expression of p53 by 094 or 117 leads to tumor growth suppression, we used a “mini-ring” 3D-tumor spheroid model. The utilization of 3D-tumor

spheroid models has been shown to reproduce the majority of the features exhibited by *in vivo* human solid tumors, including resistance to therapeutics[32]. We found that both 094 and 117 decreased RKO spheroid cell viability in a dose-dependent manner (Fig. 5A–B).

It is widely recognized that DNA-damage inducing chemotherapeutics, such as doxorubicin, enhance p53 expression[33]. Therefore, we asked if 094 or 117 enhance doxorubicin-mediated p53 induction. We found that γ-H2AX, which can be used to measure the extent of DNA damage response[34], and p53 were induced by treatment with doxorubicin in wild-type and RBM24/38-null RKO cells as expected (Fig. 5C, left and middle panels). However, treatment of compound 094 or 117 alone was able to induce γ-H2AX in wild-type but not RBM24/38-null or p53-null RKO cells (Fig. 5C, middle and right panels), suggesting that compounds 094 and 117 have no intrinsic ability to induce DNA damage. Importantly, we found that 094 and 117 were highly potent to enhance doxorubicin-mediated induction of p53 and γ-H2AX in wild-type but not RBM24/RBM38-null and p53-null RKO cells (Fig. 5C). Additionally, 094 and 117 increased the accumulation of both cleaved PARP and caspase 3 when treated alone, and further increased their accumulation when treated concurrently with doxorubicin, suggesting that these compounds are eliciting an apoptotic response (Supp. Fig. 4)[35]. To determine if compounds 094 and 117 can sensitize tumor cells to doxorubicin, we performed a cell viability assay in 3D-tumor spheroids treated with compound 094 or 117 alone, or concurrently with doxorubicin. Our data showed that both 094 and 117, alone or together with doxorubicin, significantly decreased tumor spheroid cell viability in wild-type cells (Fig. 5D–E). We would like to note that compound 117 retained growth-suppressing activity alone, and in combination with doxorubicin, in both RBM24/38-null and p53-null cells (Fig. 5D–E). These data suggest that compound 117 may have an off-target cytotoxicity.

eIF4E hyperactivity is being targeted in the clinic by utilizing small molecule inhibitors, such as 4EGI-1, to block its ability to interact with eIF4G, limiting the translation of oncogenic transcripts[36]. Therefore, we asked if compound 094 could enhance the effect of 4EGI-1. We showed that tumor cell viability was decreased by treatment of 4EGI-1 alone in wild-type RKO and HCT116 cells, RBM24/38-null and p53-null RKO cells, and eIF4E Δ-Cterm HCT116 cells (Fig. 5F, and Supp. Fig. 5). We would like to mention that the cells were treated with 10 μM 4EGI-1, which is not a concentration high enough to inhibit all cap-dependent translation[14]. We also showed that the ability of 4EGI-1 to suppress cell viability was enhanced by compound 094 in wild-type RKO and HCT116 cells, but not in RBM24/38-null and p53-null RKO cells and eIF4E Δ-Cterm HCT116 cells (Fig. 5F, and Supp. Fig. 5). Together, these data support that 094 may be explored as an adjuvant with doxorubicin or 4EGI-1 for cancers that harbor wild-type p53 (Fig. 6).

Discussion

Clinically, enhanced expression of eIF4E is correlated with increasing grade of disease[37–41]. However, the full picture of how eIF4E and the eIF4F complex induce oncogenic transformation and how to target this eIF4E axis is still being drawn. As eIF4E hyperactivity selectively activates a subset of mRNAs from diverse oncogenic pathways that contribute to tumorigenesis, it comes as no surprise that eIF4E is a promising target for therapeutics

that offset pathological eIF4E activity. Various modalities have been explored, including m^7G cap inhibitors, short interfering RNAs, antisense oligonucleotides, and small molecule eIF4E-eIF4G inhibitors, such as 4EGI-1. These approaches have been shown to decrease the translation of oncogenic transcripts leading to decreased tumor cell growth in preclinical and clinical trials[11,42,43]. Contrastingly, our group has focused on enhancing the translation of the tumor suppressor p53 to counter the tumorigenic effect of the oncogenic protein expression selected through enhanced eIF4E activity as a potential therapeutic approach.

We identified compound 094 as a first-in-class inhibitor of the eIF4E-RBM38 complex. Mechanistically, 094 binds to a previously undrugged C-terminal pocket in eIF4E abrogating the ability for RBM38 to bind, enhancing p53 mRNA translation (Figs. 1–3, and 6). However, it is still yet to be determined if 094 disrupts the eIF4E-RBM38 complex, or merely inhibits its formation. To test the specificity of 094, we used multiple CRISPR/Cas9 generated knockout and knockin cell lines. We showed that compound 094 was unable to induce p53 expression or decrease tumor cell viability in RBM24/38 double knockout or p53-null RKO cell lines treated alone or in combination with doxorubicin. In addition, we confirmed that the ability of 094 to enhance p53 protein expression and suppress tumor cell growth was dependent on its ability to interact with the C-terminal pocket within eIF4E. Substitution of eIF4E aspartic acid 202 with a positively charged lysine, or deletion of the last 17 amino acids in eIF4E, which makes up the 094-binding pocket, abrogated the ability for 094 to function (Figs. 3 and 5, Supp. Figs. 1 and 5).

Therapeutically, we demonstrated that 094 increases p53 protein expression alone, and further enhances doxorubicin-mediated p53 induction (Fig. 5). p53 expression and apoptosis have both been shown to enrich γ-H2AX (a marker of DNA damage)[34,44,45]. As compound 094 was not able to enhance γ-H2AX in p53-null cells, the data support that compound 094 has no intrinsic ability to induce DNA damage. In line with enhanced p53 expression, 094 treatment alone, or in combination with doxorubicin enhanced apoptosis and suppressed 3D tumor spheroid growth (Fig. 5). Further, we showed that 094 was able to enhance the tumor suppressive abilities of 4EGI-1, a potent inhibitor of the eIF4E-eIF4G interaction. 4EGI-1 has been shown to be effective at decreasing the translation of pro-oncogenic transcripts leading to decreased tumor cell growth[5,16]. However, since elevated expression of eIF4G, or treatment with 4EGI-1 can promote cap-independent translation, the possibility that compound 094 may not only increase p53 cap-dependent translation, but also p53 cap-independent translation should be explored in the future[46,46].

To identify key structural components to aid in the discovery of more potent eIF4E-RBM38 inhibitors, we performed a structure-activity relationship (SAR) study. Of the 15 analogs screened, only compound 117 retained activity similar to our initial lead compound 094 (Supp. Fig. 3B). This initial SAR demonstrated that both the fluorobenzene and ethyl benzamide are important for activity. However, while compound 117 showed specificity in enhancing p53 protein expression in an RBM24/38-dependent manner (Fig. 5C), our subsequent 3D tumor spheroid cell viability assays demonstrated that 117 retained activities in both RBM24/38- and p53-null RKO cells when treated alone or in combination with doxorubicin (Fig. 5D–E). These data lead us to believe that compound 117 may have off

target effects, such as cell cycle arrest, but not apoptosis (Supp. Fig. 4), which needs to be further explored.

Collectively, we identified compound 094 as a first-in-class inhibitor of the eIF4E-RBM38 complex capable of enhancing wild-type p53 expression and sensitizing 3D tumor spheroids to doxorubicin treatment. Furthermore, we showed that compound 094 enhanced the tumor suppressive abilities of small molecule 4EGI-1. Our data suggest that two distinct approaches can be used to modulate eIF4E activity for cancer therapy: (1) by suppressing eIF4E translation of "weak" oncogenic transcripts (4EGI-1); (2) by enhancing the translation of the tumor suppressor p53 (094) for cancers that harbor wild-type p53 expression.

Supplementary Material

Refer to Web version on PubMed Central for supplementary material.

Acknowledgement

We would like to thank Drs. Ting Wang and Duan Yong (Department of Biomedical Engineering, University of California, Davis) for performing the initial *in-silico* docking of the ZINC database. We are very appreciative of the help by Dr. Diego R. Yankelevich (Department of Electrical and Computer Engineering, University of California, Davis) who provided his time and support with the UV light source needed for the photoaffinity assay.

Financial support:

RO1 CA250338, RO1 CA224433, T32 CA108459, UCD CCAH 2021-27-F, UCD CCAH 2020-15-F

References

1. Rau M, Ohlmann T, Morley SJ, Pain VM. A reevaluation of the Cap-binding protein, eIF4E, as a rate-limiting factor for initiation of translation in reticulocyte lysate. Journal of Biological Chemistry. 1996;271:8983–90. [PubMed: 8621544]
2. Duncan R, Milburn SC, Hershey JWB. Regulated phosphorylation and low abundance of HeLa cell initiation factor eIF-4F suggest a role in translational control. Heat shock effects on eIF-4F. Journal of Biological Chemistry. 1987;
3. Piserà A, Campo A, Campo S. Structure and functions of the translation initiation factor eIF4E and its role in cancer development and treatment. Journal of Genetics and Genomics. Elsevier; 2018;45:13–24.
4. Hsieh AC, Ruggero D. Targeting eukaryotic translation initiation factor 4E (eIF4E) in cancer. Clinical Cancer Research. American Association for Cancer Research; 2010;16:4914–20.
5. Romagnoli A, D'Agostino M, Ardiccioni C, Maracci C, Motta S, La Teana A, et al. Control of the eIF4E activity: structural insights and pharmacological implications. Cellular and Molecular Life Sciences. Springer; 2021;78:6869.
6. De Benedetti A, Graff JR. eIF-4E expression and its role in malignancies and metastases. Oncogene. 2004/04/20. Department of Biochemistry and Molecular Biology, Louisiana State University Medical Center, Shreveport, 1501 Kings Highway, PO Box 33932, Shreveport, LA 71130, USA. adeben@lsuhsc.edu; 2004;23:3189–99.
7. Coleman LJ, Peter MB, Teall TJ, Brannan RA, Hanby AM, Honarpisheh H, et al. Combined analysis of eIF4E and 4E-binding protein expression predicts breast cancer survival and estimates eIF4E activity. British Journal of Cancer 2009 100:9. Nature Publishing Group; 2009;100:1393–9.
8. Siddiqui N, Sonenberg N. Signalling to eIF4E in cancer. Biochem Soc Trans. Portland Press Ltd; 2015;43:763.
9. Carroll M, Borden KLB. The Oncogene eIF4E: Using Biochemical Insights to Target Cancer. Journal of Interferon & Cytokine Research. Mary Ann Liebert, Inc.; 2013;33:227.

10. Feoktistova K, Tuvshintogs E, Do A, Fraser CS. Human eIF4E promotes mRNA restructuring by stimulating eIF4A helicase activity. Proc Natl Acad Sci U S A. Proc Natl Acad Sci U S A; 2013;110:13339–44. [PubMed: 23901100]
11. Pelletier J, Graff J, Ruggero D, Sonenberg N. TARGETING THE eIF4F TRANSLATION INITIATION COMPLEX: A CRITICAL NEXUS FOR CANCER DEVELOPMENT. Cancer Res. NIH Public Access; 2015;75:250.
12. Li S, Jia Y, Jacobson B, McCauley J, Kratzke R, Bitterman PB, et al. Treatment of breast and lung cancer cells with a N-7 benzyl guanosine monophosphate tryptamine phosphoramidate pronucleotide (4Ei-1) results in chemosensitization to gemcitabine and induced eIF4E proteasomal degradation. Mol Pharm. Mol Pharm; 2013;10:523–31. [PubMed: 23289910]
13. Ghosh B, Benyumov AO, Ghosh P, Jia Y, Avdulov S, Dahlberg PS, et al. Nontoxic chemical interdiction of the epithelial-to-mesenchymal transition by targeting cap-dependent translation. ACS Chem Biol. ACS Chem Biol; 2009;4:367–77. [PubMed: 19351181]
14. Moerke NJ, Aktas H, Chen H, Cantel S, Reibarkh MY, Fahmy A, et al. Small-Molecule Inhibition of the Interaction between the Translation Initiation Factors eIF4E and eIF4G. Cell. Elsevier B.V; 2007;128:257–67.
15. Fan S, Li Y, Yue P, Khuri FR, Sun SY. The eIF4E/eIF4G interaction inhibitor 4EGI-1 augments TRAIL-mediated apoptosis through c-FLIP Down-regulation and DR5 induction independent of inhibition of cap-dependent protein translation. Neoplasia. Neoplasia; 2010;12:346–56. [PubMed: 20360945]
16. Lu C, Makala L, Wu D, Cai Y. Targeting translation: eIF4E as an emerging anticancer drug target. Expert Rev Mol Med. Cambridge University Press; 2016;18.
17. Zhang J, Cho SJ, Shu L, Yan W, Guerrero T, Kent M, et al. Translational repression of p53 by RNPC1, a p53 target overexpressed in lymphomas. Genes Dev. Comparative Cancer Center, Schools of Medicine and Veterinary Medicine, University of California at Davis, USA.; 2011;25:1528–43.
18. Lucchesi CA, Zhang J, Ma B, Chen M, Chen X. Disruption of the RBM38-eIF4E complex with a synthetic peptide PEP8 increases p53 expression. Cancer Res. 2019;
19. Lucchesi CA, Zhang J, Vasilatis DM, Yip E, Chen X. Optimization of eIF4E-Binding Peptide Pep8 to Disrupt the RBM38-eIF4E Complex for Induction of p53 and Tumor Suppression. Front Oncol. Frontiers Media S.A; 2022;12:1856.
20. Aylon Y, Oren M. New plays in the p53 theater. Curr Opin Genet Dev. 2011.
21. Sun W, Laubach K, Lucchessi C, Zhang Y, Chen M, Zhang J, et al. Fine-tuning p53 activity by modulating the interaction between eukaryotic translation initiation factor eIF4E and RNA-binding protein RBM38. Genes Dev [Internet]. Genes Dev; 2021 [cited 2022 Jan 2];35:542–55. Available from: https://pubmed.ncbi.nlm.nih.gov/33664057/ [PubMed: 33664057]
22. Zhang M, Zhang J, Chen X, Cho SJ, Chen X. Glycogen synthase kinase 3 promotes p53 mRNA translation via phosphorylation of RNPC1. Genes Dev. Comparative Oncology Laboratory, University of California at Davis, Davis, California 95616, USA.; 2013;27:2246–58.
23. Kumar AB, Tipton JD, Manetsch R. 3-Trifluoromethyl-3-aryldiazirine photolabels with enhanced ambient light stability. Chemical Communications. The Royal Society of Chemistry; 2016;52:2729–32.
24. Zhang M, Xu E, Zhang J, Chen X. PPM1D phosphatase, a target of p53 and RBM38 RNA-binding protein, inhibits p53 mRNA translation via dephosphorylation of RBM38. Oncogene. 2015/03/31. Comparative Oncology Laboratory, Department of Surgical & Radiological Sciences, School of Veterinary Medicine, University of California, Davis, Davis, CA, USA.; 2015;34:5900–11.
25. Schindelin J, Arganda-Carreras I, Frise E, Kaynig V, Longair M, Pietzsch T, et al. Fiji: an open-source platform for biological-image analysis. Nat Methods. 2012/06/30. Max Planck Institute of Molecular Cell Biology and Genetics, Dresden, Germany.; 2012;9:676–82.
26. Lucchesi CA, Zhang J, Ma B, Nussinov R, Chen X. Survivin Expression is Differentially Regulated by a Selective Crosstalk between Rbm38 and miRNAs let-7b or miR-203a. Cancer Res [Internet]. American Association for Cancer Research; 2021 [cited 2021 Jan 24];canres.3157.2020. Available from: http://cancerres.aacrjournals.org/lookup/doi/10.1158/0008-5472.CAN-20-3157

27. Phan N, Hong JJ, Tofig B, Mapua M, Elashoff D, Moatamed NA, et al. A simple high-throughput approach identifies actionable drug sensitivities in patient-derived tumor organoids. Commun Biol. 2019;
28. Min Zhang Enshun Xu, Shakur Mohibi, Danielle Michelle de Anda, Yuqian Jiang, Jin Zhang, Xinbin Chen YZ. Rbm24, a target of p53, is necessary for proper expression of p53 and heart development . Cell Death Differ. 2017;
29. Sterling T, Irwin JJ. ZINC 15--Ligand Discovery for Everyone. J Chem Inf Model. 2015/10/20. Department of Pharmaceutical Chemistry, University of California, San Francisco , Byers Hall, 1700 4th Street, San Francisco, California 94158–2330, United States.; 2015;55:2324–37.
30. Lipinski CA, Lombardo F, Dominy BW, Feeney PJ. Experimental and computational approaches to estimate solubility and permeability in drug discovery and development settings. Adv Drug Deliv Rev. Elsevier; 1997;23:3–25.
31. Kumar AB, Tipton JD, Manetsch R. 3-Trifluoromethyl-3-aryldiazirine photolabels with enhanced ambient light stability. Chemical Communications. The Royal Society of Chemistry; 2016;52:2729–32.
32. Nunes AS, Barros AS, Costa EC, Moreira AF, Correia IJ. 3D tumor spheroids as in vitro models to mimic in vivo human solid tumors resistance to therapeutic drugs. Biotechnol Bioeng. 2019.
33. Lakin ND, Jackson SP. Regulation of p53 in response to DNA damage. Oncogene. Wellcome Trust/Cancer Research Campaign, Institute of Cancer and Developmental Biology, Cambridge University, Tennis Court Road, Cambridge CB2 1QR, UK.; 1999;18:7644–55.
34. Burma S, Chen BP, Murphy M, Kurimasa A, Chen DJ. ATM Phosphorylates Histone H2AX in Response to DNA Double-strand Breaks. Journal of Biological Chemistry. 2001;
35. Porter AG, Ja RU, Nicke È. Emerging roles of caspase-3 in apoptosis.
36. Sekiyama N, Arthanari H, Papadopoulos E, Rodriguez-Mias RA, Wagner G, Léger-Abraham M. Molecular mechanism of the dual activity of 4EGI-1: Dissociating eIF4G from eIF4E but stabilizing the binding of unphosphorylated 4E-BP1. Proc Natl Acad Sci U S A. National Academy of Sciences; 2015;112:E4036–45.
37. Graff JR, Konicek BW, Lynch RL, Dumstorf CA, Dowless MS, Mcnulty AM, et al. eIF4E activation is commonly elevated in advanced human prostate cancers and significantly related to reduced patient survival. Cancer Res. Cancer Res; 2009;69:3866–73. [PubMed: 19383915]
38. Coleman LJ, Peter MB, Teall TJ, Brannan RA, Hanby AM, Honarpisheh H, et al. Combined analysis of eIF4E and 4E-binding protein expression predicts breast cancer survival and estimates eIF4E activity. Br J Cancer. Br J Cancer; 2009;100:1393–9. [PubMed: 19367274]
39. Wang R, Geng J, Wang J hua, Chu X yuan, Geng H cheng, Chen L bang. Overexpression of eukaryotic initiation factor 4E (eIF4E) and its clinical significance in lung adenocarcinoma. Lung Cancer. Lung Cancer; 2009;66:237–44. [PubMed: 19261348]
40. Salehi Z, Mashayekhi F, Shahosseini F. Significance of eIF4E expression in skin squamous cell carcinoma. Cell Biol Int. Cell Biol Int; 2007;31:1400–4. [PubMed: 17689990]
41. Wang S, Rosenwald IB, Hutzler MJ, Pihan GA, Savas L, Chen JJ, et al. Expression of the eukaryotic translation initiation factors 4E and 2alpha in non-Hodgkin's lymphomas. Am J Pathol. Am J Pathol; 1999;155:247–55. [PubMed: 10393856]
42. De A, Jacobson BA, Peterson MS, Stelzner ME, Jay-Dixon J, Kratzke MG, et al. Inhibition of oncogenic cap-dependent translation by 4EGI-1 reduces growth, enhances chemosensitivity and alters genome-wide translation in non-small cell lung cancer.
43. Duffy AG, Makarova-Rusher OV., Ulahannan SV, Rahma OE, Fioravanti S, Walker M, et al. Modulation of tumor eIF4E by antisense inhibition: A phase I/II translational clinical trial of ISIS 183750-an antisense oligonucleotide against eIF4E-in combination with irinotecan in solid tumors and irinotecan-refractory colorectal cancer. Int J Cancer. Int J Cancer; 2016;139:1648–57. [PubMed: 27194579]
44. Chiu SJ, Lee YJ, Hsu TS, Chen WS. Oxaliplatin-induced gamma-H2AX activation via both p53-dependent and -independent pathways but is not associated with cell cycle arrest in human colorectal cancer cells. Chem Biol Interact. 2009;182:173–82. [PubMed: 19735649]
45. Lu C, Zhu F, Cho Y-Y, Tang F, Zykova T, Ma W-Y, et al. Cell Apoptosis: Requirement of H2AX in DNA Ladder Formation but not for the Activation of Caspase-3.

46. Moerke NJ, Aktas H, Chen H, Cantel S, Reibarkh MY, Fahmy A, et al. Small-molecule inhibition of the interaction between the translation initiation factors eIF4E and eIF4G. Cell [Internet]. Cell; 2007 [cited 2022 Dec 4];128:257–67. Available from: https://pubmed.ncbi.nlm.nih.gov/17254965/ [PubMed: 17254965]

47. Ji B, Harris BR, Liu Y, Deng Y, Gradilone SA, Cleary MP, et al. Targeting IRES-Mediated p53 Synthesis for Cancer Diagnosis and Therapeutics. Int J Mol Sci [Internet]. Department of Hepatobiliary and Pancreatic Surgery, the First Hospital of Jilin University, Changchun 130021, China. bji@hi.umn.edu. The Hormel Institute, University of Minnesota, 801 16th Avenue NE, Austin, MN 55912, USA. bji@hi.umn.edu. The Hormel Insti; 2017;18. Available from: https://www.ncbi.nlm.nih.gov/pubmed/28054974

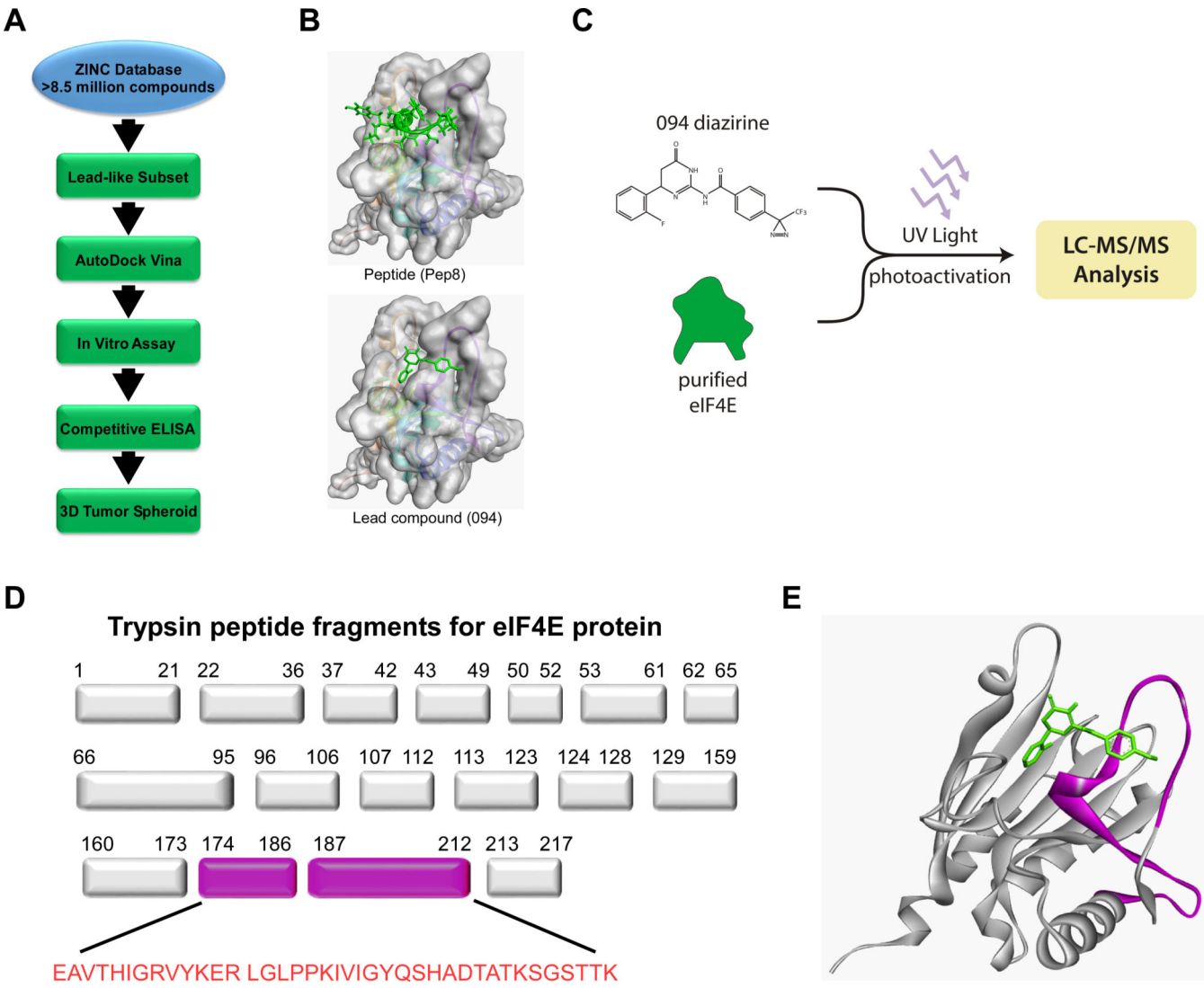

Figure 1. Identification of compound 094.

(A) Visual schematic of the workflow used to identify compound 094. (B) Visualization of the binding mode for Pep8 peptide and compound 094 to eIF4E protein c-terminal pocket determined by replica exchange molecular dynamics and AutoDock Vina. (C) Visual schematic for the workflow for the photoaffinity assay to identify the binding interface for 094 to eIF4E using a 094 photoprobe (diazirine) followed by LC-MS/MS. (D, E) Visualization of the trypsin peptide fragments identified by photoaffinity assay and LC-MS/MS indicating the binding site of compound 094 to eIF4E.

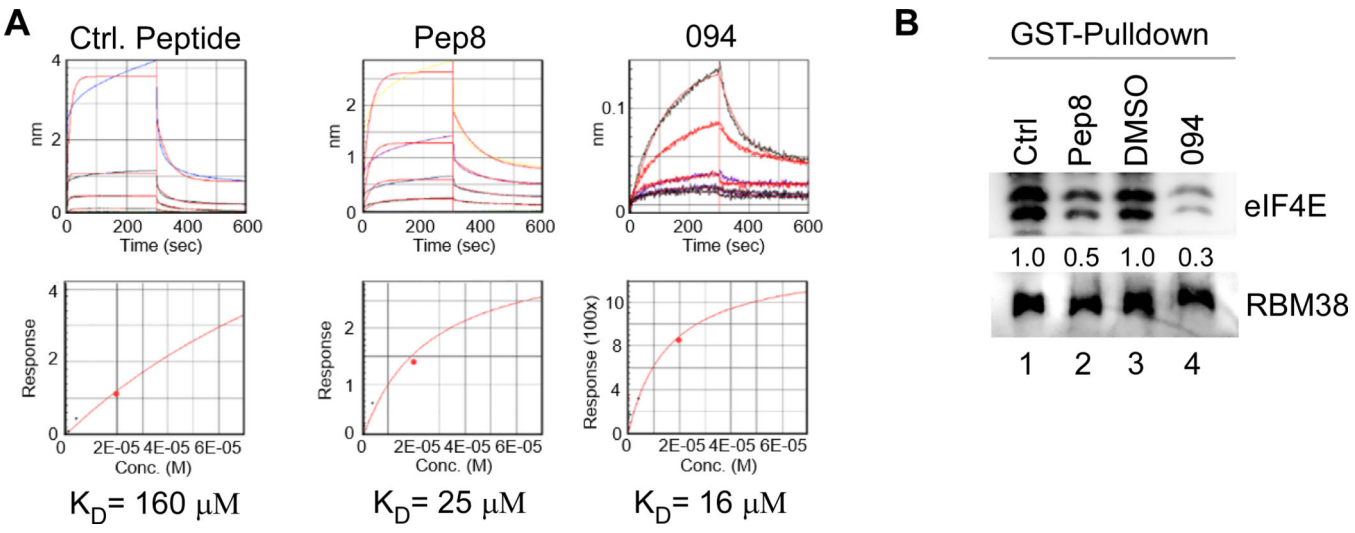

Figure 2. Compound 094 dissociates RBM38 from eIF4E.

(A) Biolayer interferometry (BLI) was used to determine the equilibrium dissociation constant (KD) for the Pep8 peptide and compound 094 to purified eIF4E. (B) Immunoblot for the competitive pull-down assay for GST-RBM38 and purified eIF4E protein in the presence of Pep8 (5mM) peptide or compound 094 (5mM). Values depict band intensity for eIF4E protein relative to peptide control (lanes 1 and 2), or DMSO control (lanes 3 and 4).

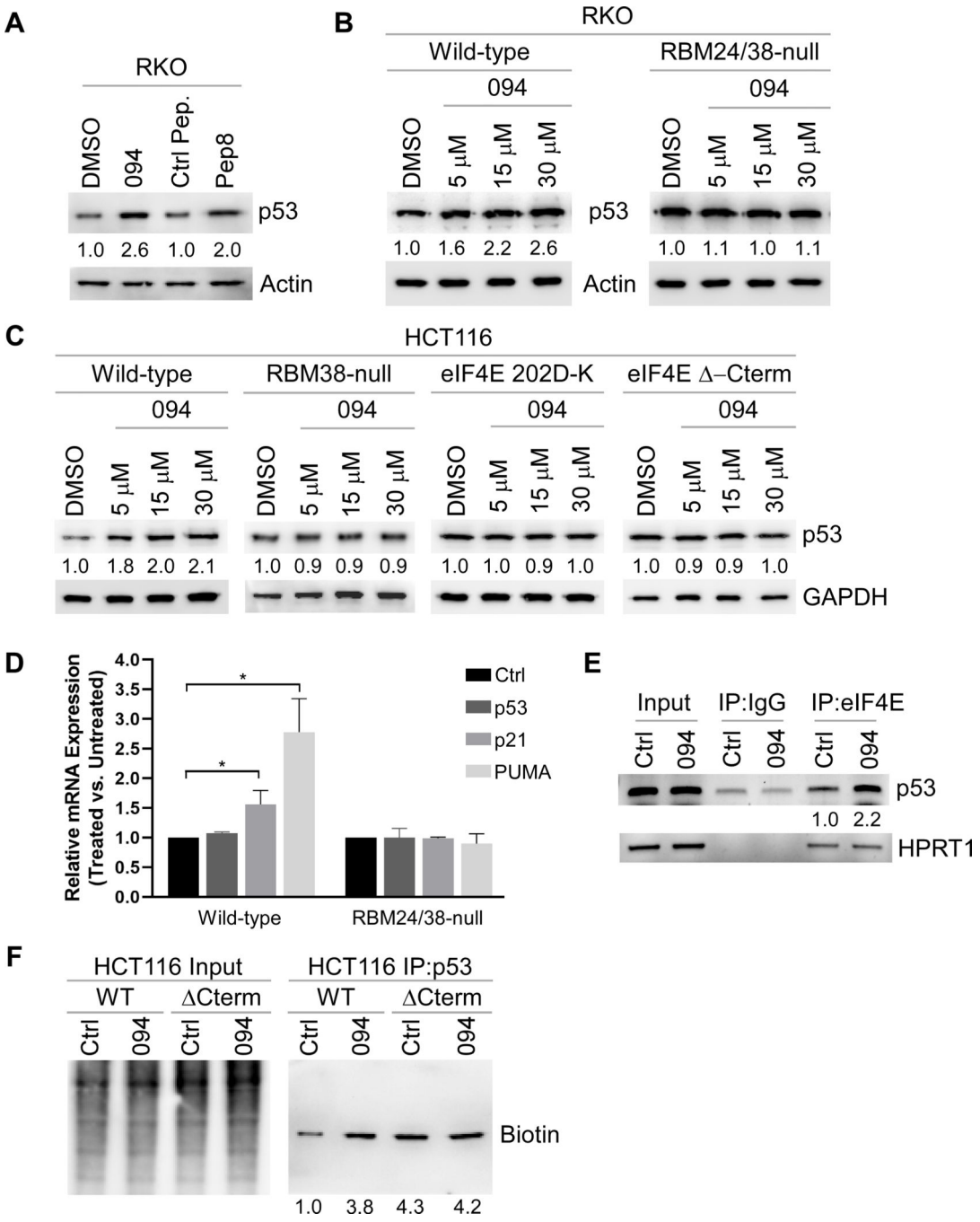

Figure 3. Compound 094 induces p53 protein expression.

(A) The protein levels of p53 and actin were measured in wild-type RKO cells treated with 094 (20 μM), Ctrl peptide (STLWDTAELWQ), or Pep8 (YPYAASPA) peptide (20 μM) for 18 hrs. (B) The protein levels of p53 and actin were measured in wild-type and RBM24/38 double knockout RKO cells treated with escalating doses of 094 for 18 hrs. (C) The protein levels of p53 and GAPDH were measured in wild-type, RBM38-null, eIF4E 202D-K mutant, and eIF4E Δ-Cterm HCT116 cells treated with escalating doses of 094 for 18 hrs. (D) The levels of p53, p21, and PUMA mRNA were measured by quantitative rt-

PCR in wild-type and RBM24/38 double knock RKO cells after treatment with 094 (20 μM) for 18 hrs. (E) RNA-ChIP assay for eIF4E binding to p53 mRNA in RKO cells treated with 094 (20 μM) for 18 hrs (values depict band intensity relative to input HPRT1 control). (F) Immunoblot for nascent p53 protein expression in wild-type and eIF4E Δ-Cterm HCT116 cells treated with 094 (10 μM) for 2 hrs (values depict band intensity relative to WT input control).

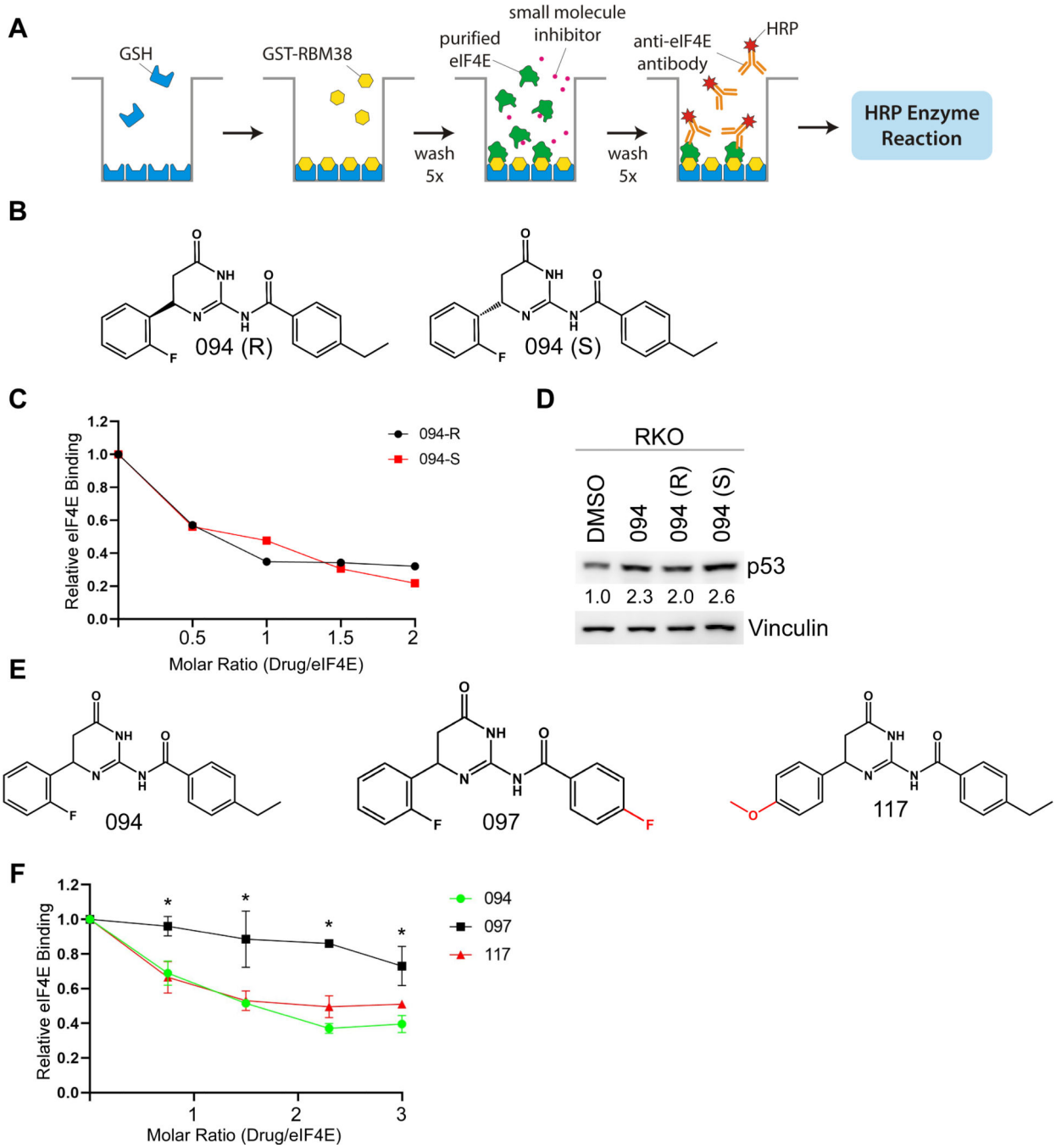

Figure 4. Structure-activity relationship of compound 094.

(A) Visual workflow for the competitive ELISA assay. (B) Chemical structures of 094 R and S enantiomers. (C) Competitive ELISA for 094 R and S enantiomers. (D) The protein levels of p53 and vinculin were measured in wild-type RKO cells treated with racemic 094, R-094, or S-094 (20 μM) for 18 hrs (values depict band intensity relative to DMSO control). (E) Chemical structures of compounds 094, 097, and 117. (F) Competitive ELISA for compounds 094, 097, and 117 (*, $P < 0.05$, relative to 094).

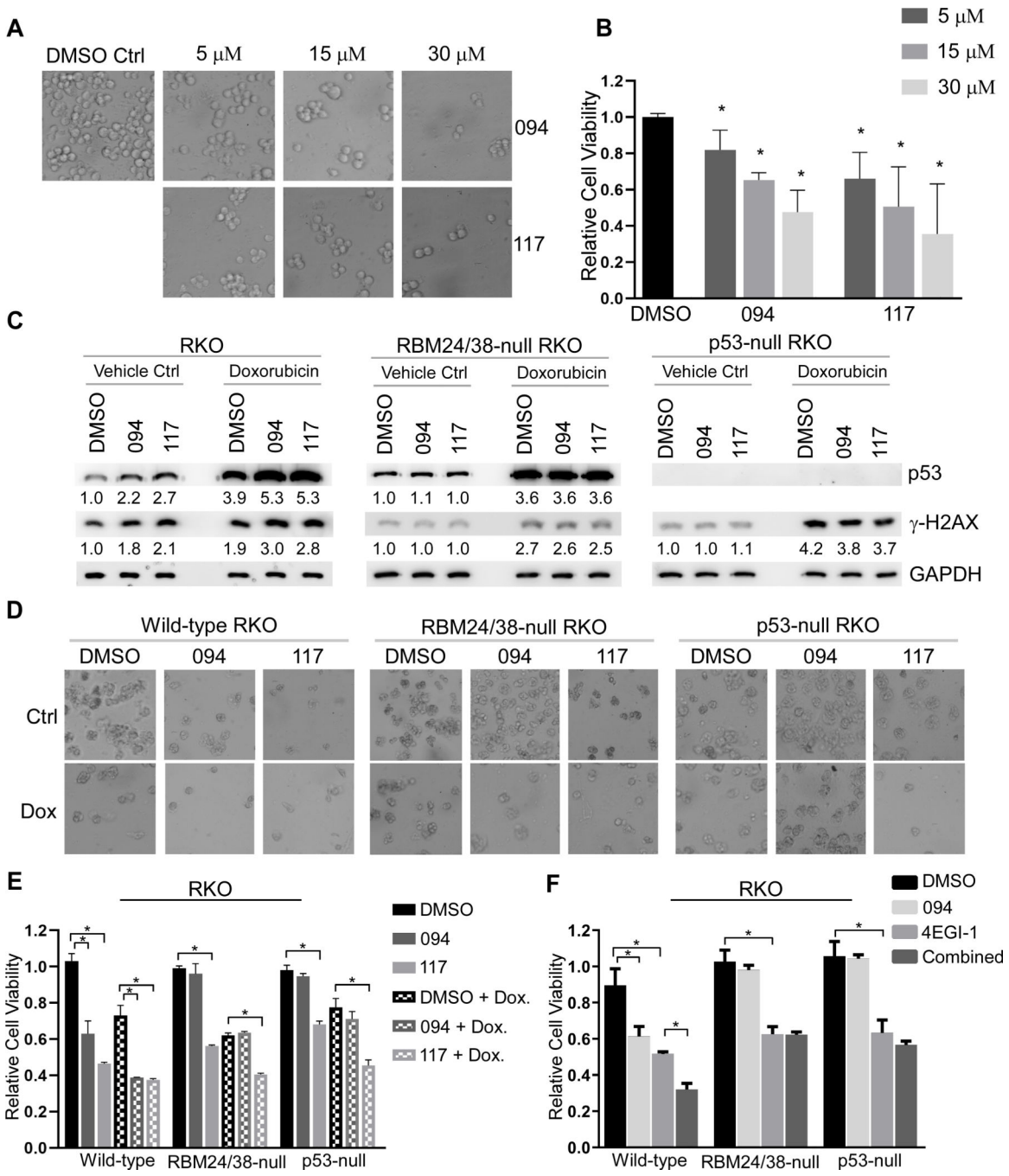

Figure 5. Compound 094 inhibits tumor cell growth and enhances doxorubicin-mediated growth suppression.

(A-B) 3D spheroid cultures and relative cell viability were measured in wild-type RKO cells after treatment with indicated dose of 094 or 117 (*, $P < 0.05$, relative to DMSO control). (C) The protein levels of p53, γ-H2AX, and GAPDH were measured in wild-type, RBM24/38 double knockout, and p53-null RKO cells after treatment with 094 or 117 alone (10 μM), or in combination with doxorubicin (3.125 ng/mL) for 18 hrs (values depict band intensity relative to DMSO control). (D-E) 3D spheroid cultures and relative cell viability were measured in wild-type, RBM24/38 double knockout, and p53-null RKO cells after

treatment with 094 or 117 alone (10 μM), or in combination with doxorubicin (3.125 ng/mL). Spheroids were imaged with a 10x microscope objective. (F) The relative cell viability was measured in wild-type, RBM24/38 double knockout, and p53-null RKO cells (2-D culture) after treatment with 094 (10 μM), 4EGI-1 (10 μM), or in combination. Values represent the mean ± SEM of three independent experiments (*, $P < 0.05$).

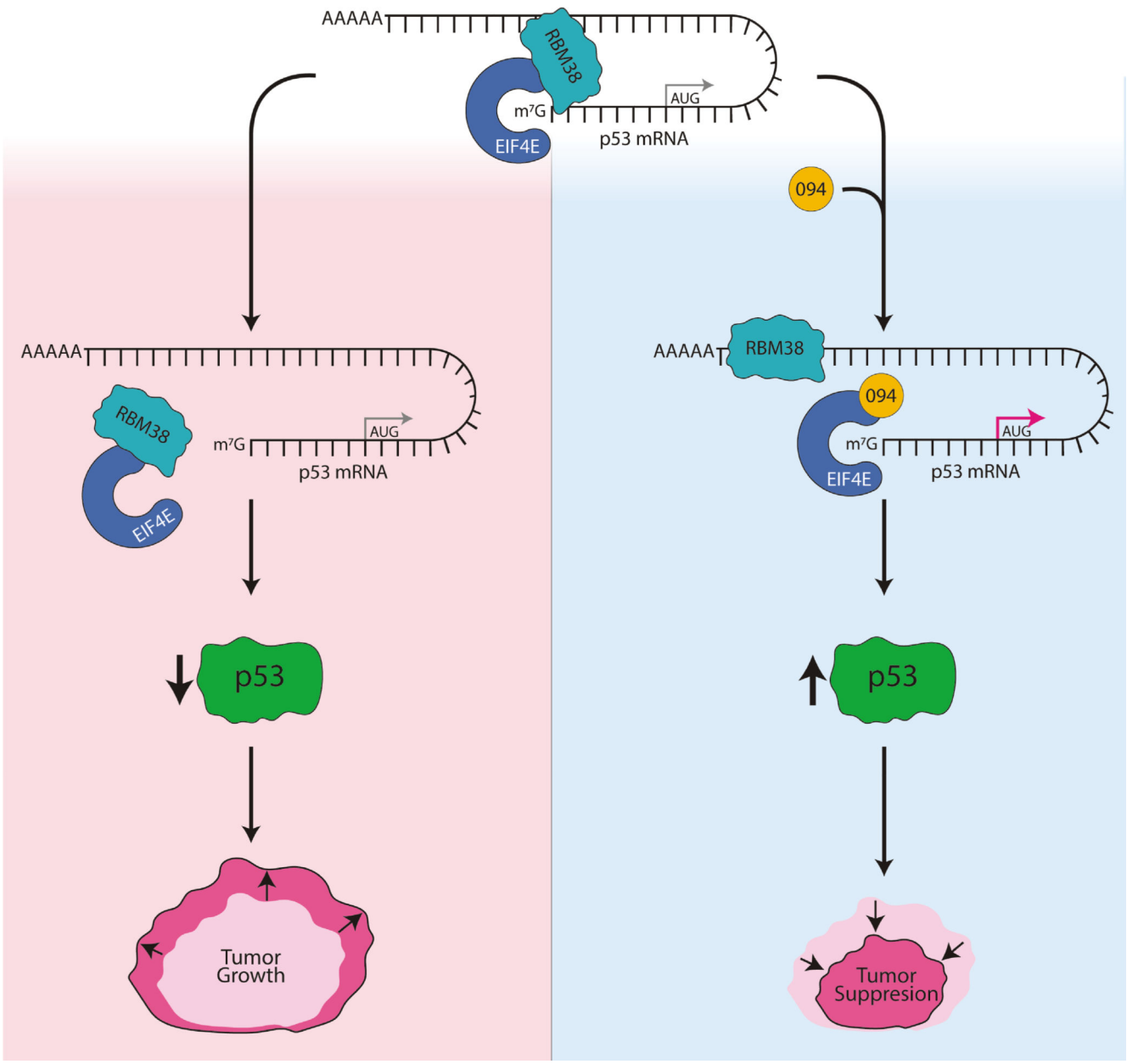

Figure 6.
Working model for how RBM38 inhibits p53 translation and the mode of action for 094 treatment.